# INTERACTION BETWEEN BENDING VIBRATIONS AND MOLECULAR ROTATION: A MODEL STUDY

Gregory S. EZRA

*Baker Laboratory, Department of Chemistry, Cornell University, Ithaca, NY 14853, USA*

The classical mechanics of the interaction between bending vibration and molecular rotation is studied for a simple rigid bender model. A one-dimensional representation of rotational motion enables surfaces of section to be constructed. Quasiperiodic, resonant and chaotic motions are identified, and related to characteristic patterns of vibration–rotation energy flow.

## 1. Introduction

The role of rotation in intramolecular dynamics is a topic of great current experimental and theoretical interest (see, for example, ref. [1] and references therein). The interaction of molecular rotation with internal vibrational motions is an important but as yet poorly understood factor in determining rates of intramolecular energy redistribution [2–8] and unimolecular decay [9–11]. The manifestations of rotation–vibration (RV) interaction are also of fundamental significance for the spectroscopy of highly excited states and weakly bound clusters [12].

Although there have been several fully quantum-mechanical calculations of RV states for realistic molecular Hamiltonians at low angular momentum $j$ (see, for example, ref. [13]), the study of high angular momentum states necessitates a classical or semiclassical approach [2–8], as the size of the RV Hamiltonian matrix to be diagonalized increases linearly with $j$. Thus, Clodius and Shirts [6] have examined the effects of rotation on the phase space structure of two coupled bonds in a model triatomic with frozen bending angle. In this case planar rotation provides an angular momentum dependent contribution to the 1 : 1 resonant interbond coupling term in the RV Hamiltonian. Both enhancement and suppression of chaos in the presence of rotation were found, depending on the relative magnitudes and

signs of the various contributions to the resonant coupling. Uzer et al. [8] have studied the role of Coriolis interactions associated with planar rotation on energy transfer between degenerate bend and asymmetric stretch modes in a model triatomic with frozen symmetric stretch coordinate. A noteworthy feature of this study is the transformation of the 1 : 1 resonance problem into a one-dimensional pendulum Hamiltonian with an angular momentum dependent barrier height. The pendulum model allows quantitative prediction of rates of energy flow, except in the regime of small non-linearity. Note that neither of the above studies considers the problem of energy flow *between* vibration and rotation. In the work of Frederick et al. [7], a detailed study of the full dynamics of rotating–vibrating triatomics (three vibrations plus rotation in three dimensions) was made from the point of view of non-linear mechanics. Both "regular" and "chaotic" RV trajectories were identified on the basis of computed Fourier transforms and rates of trajectory divergence, and trajectory character explored as a function of initial condition. In many instances chaotic trajectories were associated with large fluctuations in the geometry of rotational motion. An important finding was the importance of centrifugal coupling in promoting intramolecular RV energy transfer, and the existence of strong coupling between molecular rotation (near-prolate) and bending vibration through a 2 : 1 reso-

nance. This resonant coupling is examined further in the present paper. Similar studies have been carried out on the RV dynamics of $Ar_3$ clusters [14].

A major difficulty in the study of the classical mechanics of RV interaction has been the lack of a comprehensible representation of molecular rotation (the rotational energy surfaces recently developed by Harter and Patterson [15] are useful devices of this type). For rotation in three dimensions, there are nominally three degrees of freedom to be followed, e.g., three Euler angles and their conjugate momenta as functions of time. However, it is important to recall that there are two constants of the motion associated with rotational motion: the magnitude of total angular momentum ($j$), and the projection of the total angular momentum onto a space-fixed ($z$-) axis. In fact, Augustin and Miller have given a canonical transformation from the Euler angle description to a representation in which the angles conjugate to $j$ and $m$ are eliminated from the rotational Hamiltonian [16], and have thereby reduced the problem of three-dimensional rotation to a single degree of freedom, namely $k$, the projection of the total angular momentum onto a molecule-fixed axis, and its conjugate angle $\chi$ (see also ref. [17]). This reduction in dimensionality opens up the possibility of obtaining a very clear representation of the interaction between overall rotation and vibration. As we point out in this paper (cf. also ref. [18]), interaction of rotation with a single (bending) vibration can be studied directly using the surface of section method.

The one-dimensional representation of rotational motion has previously been exploited by Colwell et al. [19] and Duchovic and Schatz [20] for semiclassical quantization of rigid asymmetric top levels, following earlier work of King [21] (see also refs. [22,23]). Frederick and McClelland [24] have used the Augustin–Miller canonical transformation in their recent work on semiclassical quantization of the rigid bender.

In the present paper we examine the classical mechanics of RV interaction in a model triatomic, in which a bending mode interacts with three-dimensional molecular rotation. In the rigid bender model used, both bond lengths are frozen, and RV coupling occurs only through the dependence of moments of inertia on the bending coordinate. There is no Coriolis coupling in this model. Nevertheless, a rich variety of dynamical behavior is found. As there are only two degrees of freedom overall, a "rotational surface of section" can be used to examine the dynamics. In this way we are able to explore the RV phase space as a function of energy and angular momentum, and to identify several types of motion characteristic of general non-linear systems: near-separable quasiperiodic, resonant quasiperiodic, and chaotic. We are also able to associate the various types of RV motion with distinctive patterns of RV energy transfer.

Frederick and McClelland [18] have very recently also investigated the classical mechanics of a rigid bender Hamiltonian for $H_2O$. These authors have developed a perturbation theory for classical frequencies valid for the low angular momentum and energy regime, and have compared these results with the exact dynamics of their model. The model Hamiltonian treated here is considered simpler than that used by Frederick and McClelland, but captures all the essential features of the centrifugal interaction between bend and rotation.

## 2. Hamiltonian

The model problem studied consists of a single bending mode of a symmetrical triatomic $AB_2$ interacting with overall molecular rotation. The Hamiltonian for such a system is

$$H_{VR} = A(q)J_z^2 + B(q)J_y^2 + CJ_x^2 + 0.5p^2 + V(q) . \quad (1)$$

Here, $J_x, J_y$ and $J_z$ are projections of the rotational angular momentum onto the molecule-fixed $x$-, $y$- and $z$-axes. The $y$-axis is taken to bisect the BAB bond angle while the $x$-axis is perpendicular to the plane of the molecule. $q$ and $p$ are the mass-weighted bending coordinate and momentum, respectively. $A(q)$, $B(q)$ and $C$ are twice the inverse moments of inertia, and $A(0) > B(0) > C$. Since the bending motion preserves $C_{2v}$ symmetry, the inertia tensor is always diagonal. For the calculations described here, we assume the simplest possible dependence (linear) of the moments of inertia on the bending coordinate:

$$2A(q) = I_z(q)^{-1}, \quad I_z(q) = I_z^0 + \alpha q , \quad (2a)$$

$$2B(q) = I_y(q)^{-1}, \quad I_y(q) = I_y^0 - \alpha q , \quad (2b)$$

$$2C = I_x^{-1}, \quad I_x = I_x^0 . \tag{2c}$$

Note that the moment of inertia perpendicular to the plane of the molecule is independent of the bending coordinate in this approximation, and that the planarity condition

$$I_z(q) + I_y(q) = I_x^0 \tag{3}$$

is maintained for all $q$. The bending potential $V(q)$ is taken to be of the form

$$V(q) = 0.5 \, \Omega^2 q^2 + \zeta q^4 . \tag{4}$$

We shall present results for $V(q)$ both *harmonic* ($\zeta = 0$) and anharmonic. (Potentials of the type (4) clearly exhibit unphysical behavior for negative $\zeta$ and large values of $|q|$. However, at the energies of the trajectories shown below, the turnover region of the potential is not reached.) While the effect of anharmonicity is certainly to increase the extent of RV coupling (see below), for high $j \approx 20$ there is considerable RV coupling even for a pure harmonic bend. A set of parameters appropriate for the molecule $H_2O$ is given in table 1. For the purpose of the present exploratory study, we regard $\alpha$ as a parameter that allows us to tune the strength of the interaction between rotation and the bending mode.

The Augustin–Miller [16] canonical transformation results in the following expressions for the body-fixed components of the angular momentum $j$:

$$J_x = -(j^2 - k^2)^{1/2} \sin \chi , \tag{5a}$$

$$J_y = -(j^2 - k^2)^{1/2} \cos \chi , \tag{5b}$$

$$J_z = k , \tag{5c}$$

where $(k, \chi)$ are the canonical variables for rotation, and $j$ is the magnitude of the total angular momentum. With the choice of $z$-axis as the axis of quantization,

Table 1
Parameters for model $H_2O$ (au)

| | |
|---|---|
| $I_x^0$ | $11.55 \times 10^3$ |
| $I_y^0$ | $7.53 \times 10^3$ |
| $I_z^0$ | $4.02 \times 10^3$ |
| $\Omega$ | $7.3 \times 10^{-3}$ |
| $\alpha$ | $35.0$ |

$k$ is approximately a conserved quantity for $k \approx j$. When the angular momentum vector $j$ is aligned along the space-fixed $z$-axis, the conjugate angle $\chi$ becomes equal to the third Euler angle $\psi$ (minus $\pi$). The final form of the Hamiltonian is

$$H_{VR} = A(q)k^2 + (j^2 - k^2)[B(q) \cos^2\chi + C \sin^2\chi]$$
$$+ 0.5 \, p^2 + V(q) . \tag{6}$$

It is clear from this expression that the rotational and vibrational degrees of freedom are coupled solely through the $q$-dependence of $A$ and $B$. The RV phase space is four-dimensional: $(\chi, q, k, p)$. The familiar Poincaré surfaces of section method [25] can therefore be used to study the dynamics of system (6). This we do in the next section.

## 3. Results

We first examine the structure of the uncoupled asymmetric rotor phase space, shown in fig. 1. This plot corresponds to setting $q = p = 0$ in the VR Hamiltonian (6), and plotting $k$ versus $\chi$. Each contour represents a rigid-rotor trajectory at a particular value of the rotational energy:
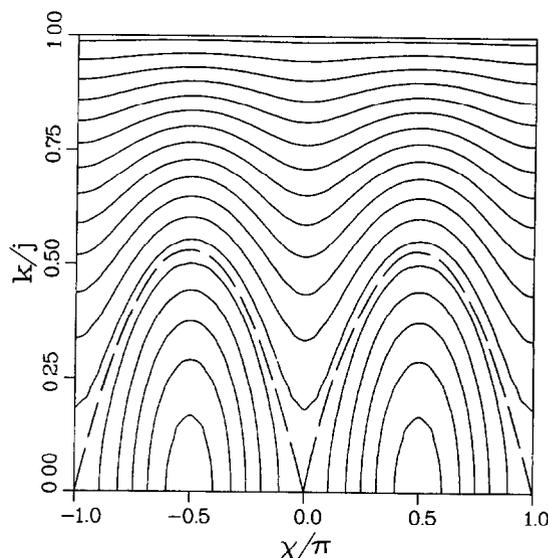


Fig. 1. Rigid-rotor phase space. This plot shows contours of the rigid-rotor Hamiltonian of eq. (7) in the $(k, \chi)$ plane. The dashed line is the separatrix dividing A- from C-type motion.

$$H_R = A(0)k^2 + (j^2 - k^2)[B(0)\cos^2\chi + C\sin^2\chi]. \quad (7)$$

Removing a constant factor $j^2$, it can be seen that the rotor Hamiltonian (7) depends on $k$ only through the ratio $k/j$, so that for a *rigid* rotor the structure of the rotational phase space is the same for all values of $j$. Note that the equations of motion and hence the rotational phase space are invariant under the transformation $k \to -k, \chi \to -\chi$, and we show only the positive $k$ half.

Three distinct types of rotational motion can be identified in fig. 1. The first, so-called A-type motion, occurs at high rotational energies and fills the upper half of the plot. It essentially corresponds to rotation of the molecule around the body-fixed $z$- or $A$-axis (detailed accounts of the classical mechanics of rigid rotors are given in refs. [15,26]). In A-type motion, the trajectory has the topology of a rotation in the angle $\chi$. The second type of motion, so-called C type, occurs at lower rotational energies for fixed $j$ and occupies the two island regions in the middle of the rotational phase space. This motion corresponds to rotation of the molecule around the molecule-fixed $x$-axis. There are two stable fixed points for C-type motion at $k = 0, \chi = \pi/2$ and $3\pi/2$. In C-type motion, the trajectory corresponds to librational motion in $\chi$. The third type of motion is called B type, and defines the separatrix dividing A- from C-type motion (shown as a dashed line in fig. 1) [15]. There are two unstable fixed points at $k = 0, \chi = 0, \pi$, corresponding to rotation around the molecule-fixed $y$-axis.

When coupling between rotation and vibration is included, a rotational surface of section can be defined by plotting $(k, \chi)$ for $q = 0, p > 0$, for trajectories of the fully coupled system at a fixed value of the total energy. A key point of the present work (see also ref. [18]) is that comparison of rotational surfaces of section with the uncoupled phase space of fig. 1 provides a very direct view of the effects of RV interaction on rotational dynamics.

In fig. 2 we show rotational surfaces of section for four trajectories with total angular momentum $j = 10$ (in units of $\hbar$; we set $j \to j + 0.5$ in the classical Hamiltonian (6), cf. ref. [19]). The trajectory in fig. 2a corresponds to a harmonic bending mode, $\zeta = 0$. At the energy shown, $E = 1.5 \times 10^{-2}$ au ($\approx 3000$ cm$^{-1}$), the rotational surface of section closely resembles the uncoupled rotational phase space and

there is clearly very little interaction between bending and vibration. This is the case for the harmonic bend with $j = 10$ throughout the range of energies we have examined, up to $E = 20000$ cm$^{-1}$. Introducing anharmonicity in the bending potential increases the extent of RV coupling at high energies. Figs. 2b, 2c show two surfaces of section with $\zeta = -2 \times 10^{-7}$ au. The first (fig. 2b) has energy $E = 8000$ cm$^{-1}$, and shows no appreciable VR coupling. The second (fig. 2c) is at $E = 17000$ cm$^{-1}$, and displays interesting structure in the surface of section. We note first the appearance of chains of islands corresponding to resonant RV trajectories. There are prominent 4 : 1 and 6 : 1 resonances (ratio of local vibrational to rotational frequencies) in the upper portion of the phase plane ("A-type resonances"). A chain of six islands, three of which are visible in the plot, appears in the region of the phase plane corresponding to C-type motion ("C-type resonances"). Another major feature of fig. 2c is the appearance of a band of RV stochasticity in the vicinity of the separatrix [25]. In addition to the resonant and chaotic regions of phase space, quasiperiodic A- and C-type motions persist at large $k$ and around the stable fixed points $k = 0, \chi = 0, \pi$, respectively. Fig. 2d shows the effect of increasing the anharmonicity to $\zeta = -5 \times 10^{-7}$ at total energy $E = 8000$ cm$^{-1}$ of fig. 2b. Resonant regions now appear.

Fig. 3 shows a sample of trajectories with larger values of the total angular momentum $j$, all of which correspond to pure harmonic bend. The trajectory of fig. 3a has $j = 20, E = 30000$ cm$^{-1}$. It can be seen that there is a region of RV chaos coexisting with both A- and C-type regular motion. Particularly striking is a 4 : 1 island chain embedded in the chaotic region: low-order RV resonances clearly serve to stabilize motion in the vicinity of elliptic fixed points corresponding to periodic orbits. The chain of six islands near the top of the plot is *not* a 6 : 1 A-type resonance. It is formed by two distinct trajectories, each of which produces a set of three islands displaced by $\pi$ with respect to the islands of the other trajectory. These two trajectories are thus symmetry breaking 3 : 1 resonances, and occur in symmetry related pairs (cf. local mode trajectories [27]). Fig. 3b shows a trajectory at the same energy with $j = 35$. The two small islands at $k \approx 9$ are the only remnants of regular C-type motion, and are formed by bifurca-
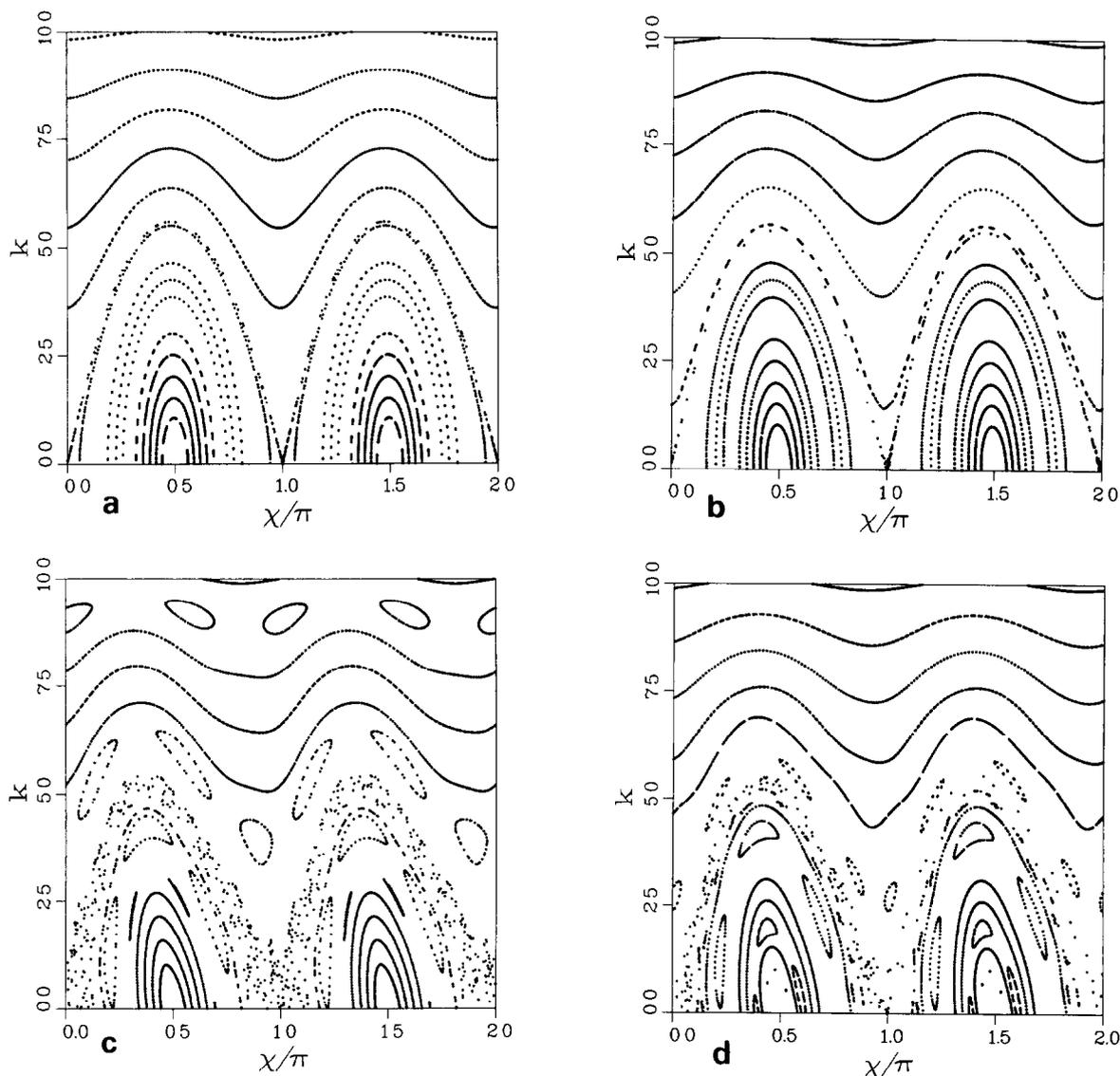
Fig. 2. Rotational surfaces of section for the rotation–vibration Hamiltonian of eq. (6), obtained by plotting $(k, \chi)$ for $q = 0$, $p > 0$, at a constant value of the energy. (a)$j = 10, E = 1.5 \times 10^{-2}, \zeta = 0.0$. (b)$j = 10, E = 4.0 \times 10^{-2}, \zeta = -2 \times 10^{-7}$. (c)$j = 10$, $E = 8.5 \times 10^{-2}, \zeta = -2 \times 10^{-7}$. (d)$j = 10, E = 4.0 \times 10^{-2}, \zeta = -5 \times 10^{-7}$.

tion of the original elliptic C-type fixed points (see below). A-type regular and chaotic motion occupy the rest of phase space.

Fig. 3c corresponds to the same values of $j$ and $E$ as 3b, but with a smaller value of the RV coupling constant $\alpha = 10.0$. The most striking feature of this plot is a large 2 : 1 A-type resonance zone, corre-

sponding to the 2 : 1 centrifugal resonances observed by Frederick et al. in their study of triatomics [7]. (The possibility of finding such RV resonances in a simple rigid bender model motivated the present work.) The complementary section in the $(p, q)$ plane is shown in fig. 3d. Regular A-type motion corresponds to low vibrational energy and hence to invariant
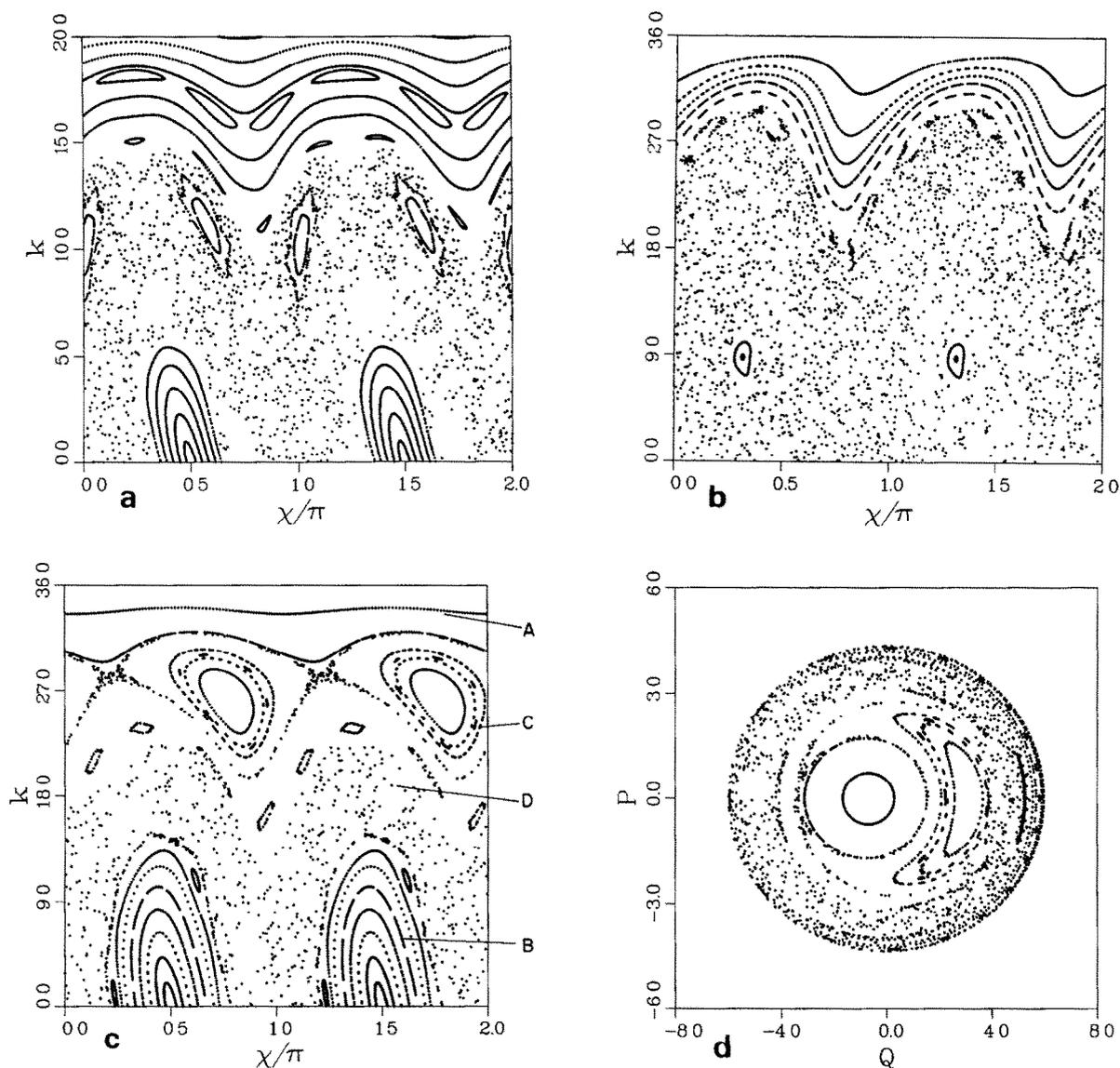
Fig. 3. Rotational surfaces of section, as for fig. 2. (a) $j = 20$, $E = 1.5 \times 10^{-1}$, $\zeta = 0$, $\alpha = 35.0$. (b) $j = 35$, $E = 1.5 \times 10^{-1}$, $\zeta = 0$, $\alpha = 35.0$. (c) $j = 35$, $E = 1.5 \times 10^{-1}$, $\zeta = 0$, $\alpha = 10.0$. (d) Complementary surface of section in $(p, q)$ plane for trajectory of (c).

curves at the center of the ellipse, whereas C-type motion corresponds to invariant curves on the outer edges of the ellipse. The 2 : 1 resonance appears in this section as the single large island off the center.

The origin of the 2 : 1 A-type resonance is easily understood qualitatively by examining the Hamiltonian (6). Expanding the inverse moment of inertia $B(q)$ to first order in $q$ gives a coupling term proportional to

$q \cos^2\chi$. In terms of zeroth-order harmonic oscillator $(J, \theta)$ and symmetric top $(k, \chi)$ action–angle variables, this coupling contains a 2 : 1 resonant term proportional to $\sin(\theta - 2\chi)$. The 2 : 1 coupling will lead to large changes in the topology of phase space when $2\omega_{rot} \approx \omega_{vib}$. Defining an averaged symmetric top rotational Hamiltonian

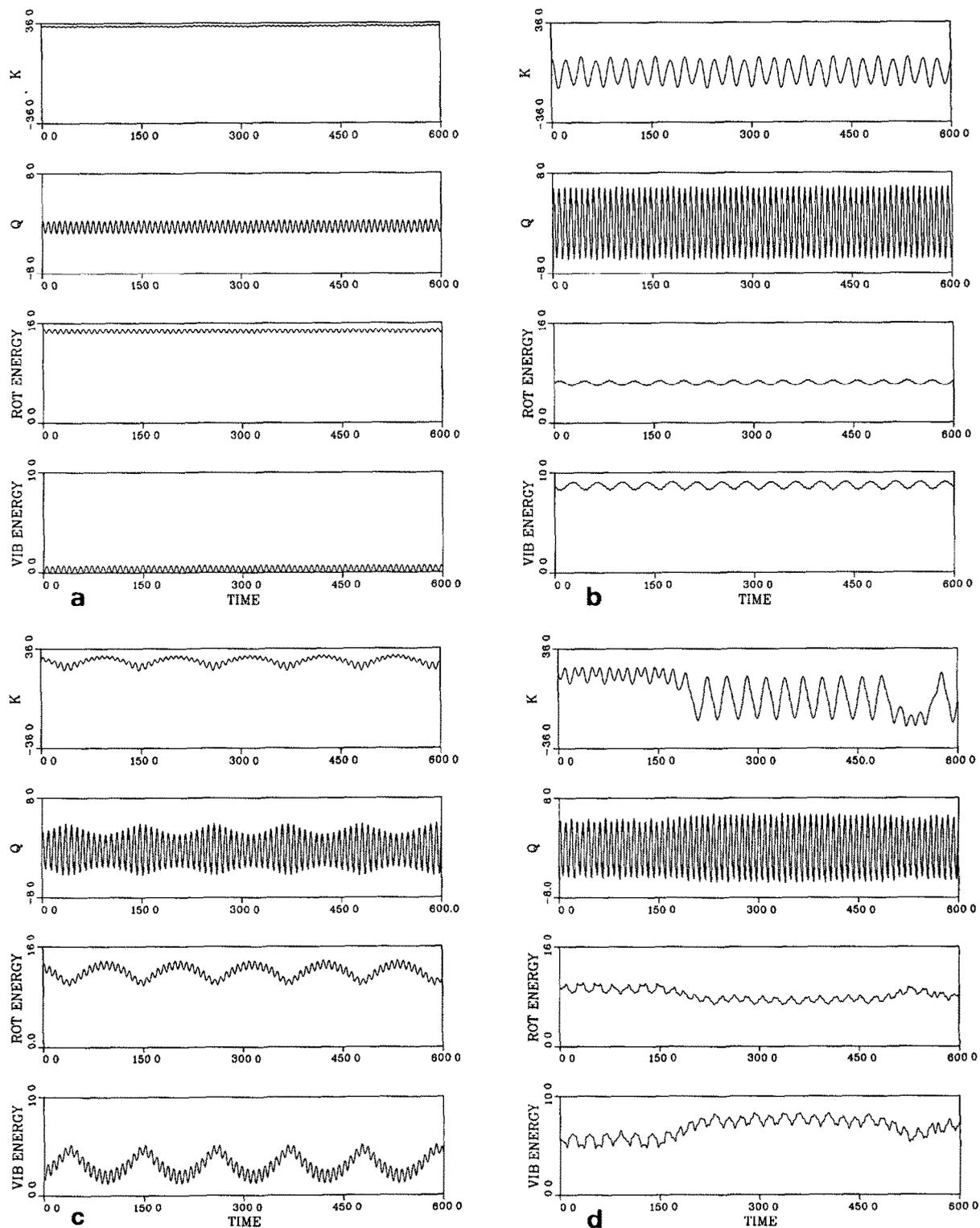$$\bar{H}_R = A(0)k^2 + 0.5(j^2 - k^2)[B(0) + C] \qquad (8)$$

Fig. 4. Plots of: $k$, $q$, $E_{rot}$ and $E_{vib}$ versus $t$ for the four trajectories A, B, C and D marked in fig. 3c.

and corresponding frequency

$$\bar{\omega}_{rot} = k[2A(0) - B(0) - C] \qquad (9)$$

leads to a value $k_{res} \approx 26$ for the center of the resonance zone, in good agreement with the value found from fig. 3c. A more quantitative analysis of RV resonances in terms of action–angle variables appropriate for an asymmetric top would of course be desirable. A treatment valid for low $E$ and $j$ has been given by Frederick and McClelland [18].

In passing from fig. 3c to fig. 3b by increasing the coupling constant $\alpha$, regular C-type motion around the fixed points $k = 0$, $\chi = \pi/2$, $3\pi/2$ disappears via a bifurcation of the islands around the fixed points which renders them unstable. This bifurcation has also been observed in the model of Frederick and McClelland [18], who comment on its significance for studies of RV interaction restricted to planar rotation.

There are several distinctive patterns of energy transfer associated with the different types of trajectory in fig. 3c. In fig. 4 we plot the following quantities versus time for the four trajectories A, B, C, and D from fig. 3c: $k$, $q$, $E_{rot}$ and $E_{vib}$, where

$$E_{rot} = A(q)k^2 + (j^2 - k^2)[B(q)\cos^2\chi + C\sin^2\chi]$$
$$\text{and} \qquad (10a)$$

$$E_{vib} = 0.5p^2 + V(q) . \qquad (10b)$$

The unit of time used here is $10^2$ au, so that the total time shown in the plots is 1.45 ps.

Fig. 4a shows an A-type regular trajectory, marked "A" in fig. 3c. For this trajectory $k$ is almost a conserved quantity, and there is no significant energy flow between rotation and vibration. Fig. 4b shows a C-type trajectory, "B" in fig. 3c. The angular momentum projection $k$ now oscillates around zero, but there is no appreciable RV energy transfer. Fig. 4c shows the resonant trajectory "C" of fig. 3c. This trajectory is clearly associated with significant periodic RV energy flow. Note that RV energy flow cannot be complete, as the amount of energy in rotation is bounded by that corresponding to extreme A- and C-type motions. Extensive intramolecular RV energy transfer was found to be associated with 2 : 1 centrifugal resonances in ref. [7]. The fourth trajectory, fig. 4d, is chaotic ("D" in fig. 3c). The variables for this trajectory exhibit an interesting time depen-

dence, which we have found for other chaotic RV trajectories: there are long-time correlations, associated with well-defined segments of the trajectory corresponding to either A- or C-type behavior of $k$. Transitions between the two types of behavior, accompanied by RV energy transfer, occur very abruptly. Such behavior is characteristic of the existence of bottlenecks in the RV phase space, which are perhaps associated with remnants of the separatrix acting as a leaky barrier to flow from high-$k$ to low-$k$ regions of phase space [28] (see also refs. [29,30]).

## 4. Discussion

We have examined the classical mechanics of a simple rigid bender model for interaction of a bending mode with three-dimensional molecular rotation. A one-dimensional representation of rotational motion [16] has enabled us to use the surfaces of section method to explore the RV phase space. Several features of the coupled RV dynamics have been characterized, including zones of RV stochasticity and prominent low-order resonances.

The approach developed here and in ref. [18] opens up many questions for future study. Thus, it would be of interest to investigate the quantum mechanics of resonant RV states. EBK quantization of the associated quasiperiodic classical motions could be achieved using a variety of methods (e.g. refs. [31, 32]). It should also be possible to identify strongly coupled resonant RV states in variational calculations of high angular momentum states of $H_2O$, either with a rigid bender model [33] or the full molecular Hamiltonian [13,34]. The question of a quantum analogue for the Miller–Augustin transformation, and hence of the rotational surface of section, is intriguing. Further non-linear resonance analysis of RV interactions in the rigid bender model using asymmetric top action–angle variables is required. Extension to triatomics in which stretching as well as bending can occur should lead to a unification with recent work on Coriolis-induced interbond energy transfer [6,8]. Finally, the effects of RV coupling on the dynamics of isomerization, in which a molecule undergoes large-amplitude low-frequency motion, remains to be explored.

## References

[1] G.M. Nathanson and G.M. McClelland, J. Chem. Phys. 81 (1984) 629.

[2] N.C. Hung and D.J. Wilson, J. Chem. Phys. 38 (1963) 828;
N.C. Hung, J. Chem. Phys. 57 (1972) 5202.

[3] C.A. Parr, A. Kupperman and R.N. Porter, J. Chem. Phys. 66 (1977) 2914.

[4] E.R. Grant and J. Santamaria, J. Phys. Chem. 85 (1981) 2426.

[5] J.A. Combs and W.G. Hoover, J. Chem. Phys. 80 (1984) 2243.

[6] W.B. Clodius and R.B. Shirts, J. Chem. Phys. 81 (1984) 6244.

[7] J.H. Frederick, G.M. McClelland and P. Brumer, J. Chem. Phys. 83 (1985) 190.

[8] T. Uzer, G.A. Natanson and J.T. Hynes, Chem. Phys. Letters 122 (1985) 12.

[9] M. Quack and J. Troe, Ber. Bunsenges. Physik. Chem. 78 (1974) 240.

[10] A.J. Stace, Ber. Bunsenges. Physik. Chem. 81 (1977) 200.

[11] J.A. Miller and N.J. Brown, J. Phys. Chem. 86 (1982) 772.

[12] R.S. Berry, in: Quantum dynamics of molecules, ed. R.G. Woolley (Plenum Press, New York, 1980).

[13] B. Maessen and M. Wolfsberg, J. Phys. Chem. 89 (1985) 3876;
C.-L. Chen, B. Maessen and M. Wolfsberg, J. Chem. Phys. 83 (1985) 1795;
J. Tennyson and B. Sutcliffe, Mol. Phys. 51 (1984) 887.

[14] L. Fried, J. Santamaria and G.S. Ezra, unpublished.

[15] W.G. Harter and C.W. Patterson, J. Chem. Phys. 80 (1984) 4241;
W.G. Harter and C.C. Kim, Am. J. Phys. 44 (1976) 1080.

[16] S.D. Augustin and W.H. Miller, J. Chem. Phys. 61 (1974) 3155.

[17] A. Deprit, Am. J. Phys. 35 (1967) 424.

[18] J. Frederick and G.M. McClelland, J. Chem. Phys. (1986), to be published.

[19] S.M. Colwell, N.C. Handy and W.H. Miller, J. Chem. Phys. 68 (1978) 745.

[20] R. Duchovic and G.C. Schatz, J. Chem. Phys. 84 (1986) 2239;
G.C. Schatz, in: Molecular collision dynamics, ed. J.M. Bowman (Springer, Berlin, 1983).

[21] G.W. King, J. Chem. Phys. 15 (1947) 820.

[22] H.A. Kramers and G.P. Ittmann, Z. Physik 53 (1929) 553; 58 (1929) 217; 60 (1930) 663.

[23] P. Pajunen, J. Chem. Phys. 83 (1985) 2363.

[24] J.H. Frederick and G.M. McClelland, J. Chem. Phys. 84 (1986) 976.

[25] A. Lichtenberg and M.A. Lieberman, Regular and stochastic motion (Springer, Berlin, 1983).

[26] H. Goldstein, Classical mechanics (Addison–Wesley, Reading, 1980).

[27] M.S. Child and L. Halonen, Advan. Chem. Phys. 57 (1984) 1.

[28] S.R. Channon and J. Lebowitz, Ann. NY Acad. Sci. 357 (1980) 108.

[29] R.S. Mackay, J.D. Meiss and I.C. Percival, Physica 13D (1984) 55;
D. Bensimon and L.P. Kadanoff, Physica 13D (1984) 82.

[30] M.J. Davis, J. Chem. Phys. 83 (1985) 1016;
M.J. Davis and S.K. Gray, preprint;
M.J. Davis, S.K. Gray and S.A. Rice, preprint.

[31] S. Skodje, M. Borondo and W.P. Reinhardt, J. Chem. Phys. 82 (1985) 4611.

[32] C.C. Martens and G.S. Ezra, J. Chem. Phys. 83 (1985) 2990.

[33] P.R. Bunker, Ann. Rev. Phys. Chem. 34 (1983) 59.

[34] J.K.G. Watson, Mol. Phys. 15 (1968) 479.